AC

cea

DAPNIA

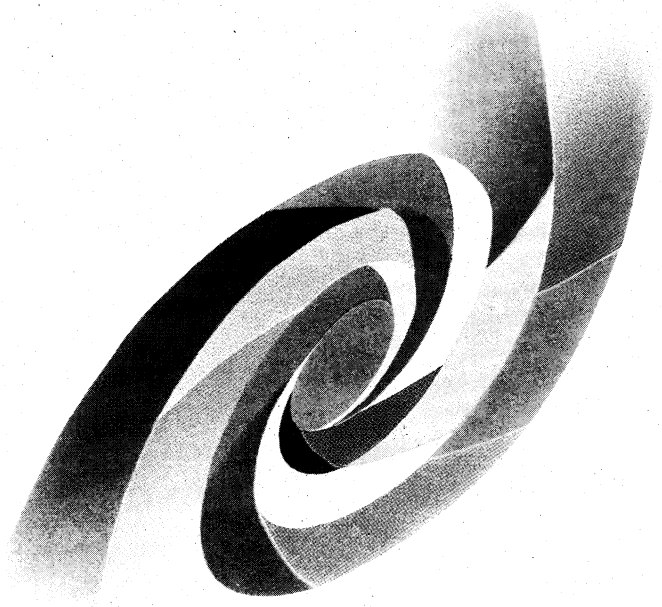

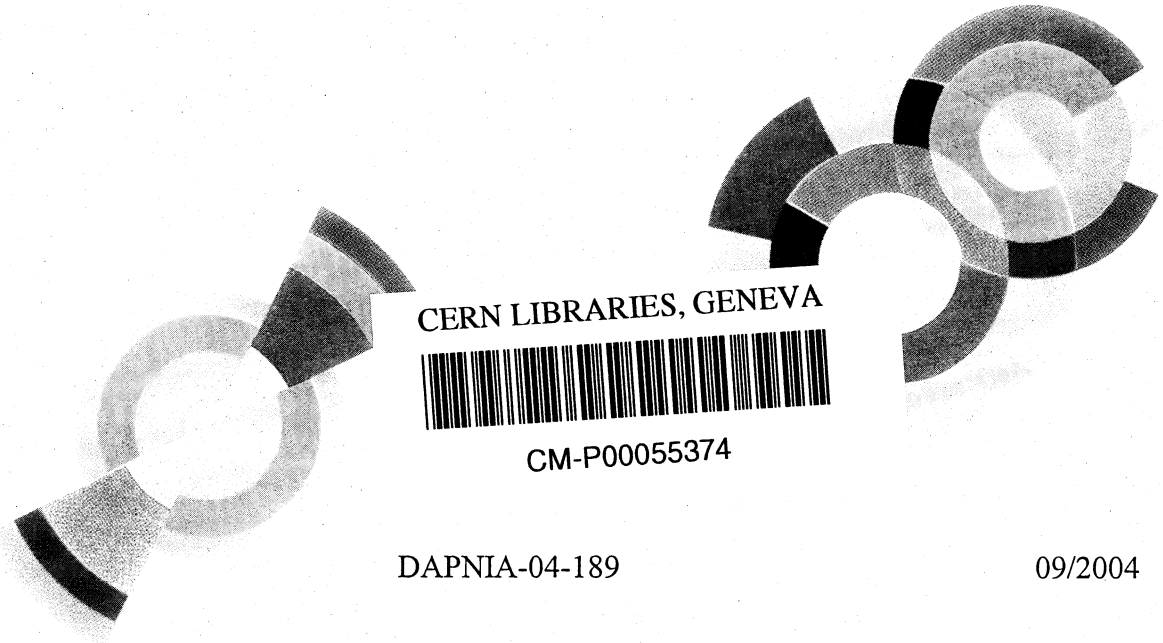

DAPNIA-04-189 09/2004

Role of the baryon resonances in the η and K^+ photoproduction processes on the proton.

B. Saghai

Talk given at the Workshop on The Physics of Excited Nucleons (NSTAR-2004), Grenoble (France), March 24-27,2004

Département d'**A**strophysique, de Physique des **P**articules, de Physique **N**ucléaire et de l'**I**nstrumentation **A**ssociée

DSM/DAPNIA, CEA/Saclay F - 91191 Gif-sur-Yvette Cédex
Tél : (1) 69 08 24 02 Fax : (1) 69 08 99 89
http : //www-dapnia.cea.fr

Couverture : Sylvie Cabrit et Marc Sauvage

ROLE OF THE BARYON RESONANCES IN THE η AND K^+ PHOTOPRODUCTION PROCESSES ON THE PROTON

B. SAGHAI
DAPNIA, DSM, CEA/Saclay, 91191 Gif-sur-Yvette, France
E-mail: bsaghai@cea.fr

Very recent η and K^+ photoproduction data on the proton from threshold up to $E_\gamma^{lab} \approx 2.6$ GeV are interpreted within a chiral constituent quark formalism, which embodies all known nucleon and hyperon resonances. Possible contributions from an additional S_{11} resonance are presented.

1. Introduction

Recent experimental and theoretical investigations on the photoproduction of mesons[1] are providing us with new insights into the baryon spectroscopy. The present manuscript is devoted to the interpretation of the processes

$$\gamma\, p \rightarrow \eta\, p\ , K^+\Lambda. \tag{1}$$

Those reactions have been widely studied *via* Effective Lagrangian Approaches (ELA) for both η-meson[2,3,4,5] and kaon[6,7,8,9,10] channels. Such studies, often based on the Feynman diagrammatic technique and embodying s-,u-, and t-channel exchanges, have produced various models differing mainly in their content of baryon resonances. The number of exchanged particles dealt with in those isobaric models is limited[11] by the number of related free parameters, which increases rapidly from 1 to 5 per resonance[12], in including resonances with spin $\geq 3/2$. Given the large number of known resonances (see Table 1), such a shortcoming renders those phenomenological approches inappropraite[14] in the search for new baryon resonances predicted by various QCD-inspired formalisms[15]. The latter topic is of special interest in the present work.

The content of our chiral constituent quark approach, based on the broken $SU(6) \otimes O(3)$ symmetry, is outlined in the next Section. Comparisons between our models and data are reported in Section 3 and concluding remarks are given in Section 4.

Table 1. Baryon resonances from PDG [13], with mass $M_{N^*} \leq 2.5$ GeV. Notations are $L_{2I\ 2J}(mass)$ and $L_{I\ 2J}(mass)$ for N^* and Y^*, respectively.

Baryon	Three & four star resonances	One & two star resonances
N^*	$S_{11}(1535)$, $S_{11}(1650)$, $P_{11}(1440)$, $P_{11}(1710)$, $P_{13}(1720)$, $D_{13}(1520)$, $D_{13}(1700)$, $D_{15}(1675)$, $F_{15}(1680)$, $G_{17}(2190)$, $G_{19}(2250)$, $H_{19}(2220)$,	$S_{11}(2090)$, $P_{11}(2100)$, $P_{13}(1900)$, $D_{13}(2080)$, $D_{15}(2200)$, $F_{15}(2000)$, $F_{17}(1990)$,
Λ^*	$S_{01}(1405)$, $S_{01}(1670)$, $S_{01}(1800)$, $P_{01}(1600)$, $P_{01}(1810)$, $P_{03}(1890)$, $D_{03}(1520)$, $D_{03}(1690)$, $D_{05}(1830)$, $F_{05}(1820)$, $F_{05}(2110)$, $G_{07}(2100)$, $H_{09}(2350)$,	$D_{03}(2325)$, $F_{07}(2020)$,
Σ^*	$S_{11}(1750)$, $P_{11}(1660)$, $P_{11}(1880)$, $P_{13}(1385)$, $D_{13}(1670)$, $D_{13}(1940)$, $D_{15}(1775)$, $F_{15}(1915)$, $F_{17}(2030)$.	$S_{11}(1620)$, $S_{11}(2000)$, $P_{11}(1770)$, $P_{11}(1880)$, $P_{13}(1840)$, $P_{13}(2080)$, $D_{13}(1580)$, $F_{15}(2070)$, $G_{17}(2100)$.

2. Theoretical Frame

The starting point of the meson photoproduction in the chiral quark model is the low energy QCD Lagrangian[16]

$$\mathcal{L} = \bar{\psi}\left[\gamma_\mu(i\partial^\mu + V^\mu + \gamma_5 A^\mu) - m\right]\psi + \ldots \tag{2}$$

where ψ is the quark field in the $SU(3)$ symmetry, $V^\mu = (\xi^\dagger\partial_\mu\xi + \xi\partial_\mu\xi^\dagger)/2$ and $A^\mu = i(\xi^\dagger\partial_\mu\xi - \xi\partial_\mu\xi^\dagger)/2$ are the vector and axial currents, respectively, with $\xi = e^{i\Pi/f}$. f is a decay constant and the field Π is a $3 \otimes 3$ matrix,

$$\Pi = \begin{vmatrix} \frac{1}{\sqrt{2}}\pi^\circ + \frac{1}{\sqrt{6}}\eta & \pi^+ & K^+ \\ \pi^- & -\frac{1}{\sqrt{2}}\pi^\circ + \frac{1}{\sqrt{6}}\eta & K^\circ \\ K^- & \bar{K}^\circ & -\sqrt{\frac{2}{3}}\eta \end{vmatrix}, \tag{3}$$

in which the pseudoscalar mesons, π, K, and η, are treated as Goldstone bosons so that the Lagrangian in Eq. (2) is invariant under the chiral transformation. Therefore, there are four components for the photoproduction

of pseudoscalar mesons based on the QCD Lagrangian,

$$\mathcal{M}_{fi} = \langle N_f|H_{m,e}|N_i\rangle + \sum_j \left\{ \frac{\langle N_f|H_m|N_j\rangle\langle N_j|H_e|N_i\rangle}{E_i+\omega-E_j} + \frac{\langle N_f|H_e|N_j\rangle\langle N_j|H_m|N_i\rangle}{E_i-\omega_m-E_j} \right\} + \mathcal{M}_T, \quad (4)$$

where $N_i(N_f)$ is the initial (final) state of the nucleon, and $\omega(\omega_m)$ represents the energy of incoming (outgoing) photons (mesons).

The pseudovector and electromagnetic couplings at the tree level are given respectively by the following standard expressions:

$$H_m = \sum_j \frac{1}{f_m}\bar{\psi}_j\gamma^j_\mu\gamma^j_5\psi_j\partial^\mu\phi_m \; ; \; H_e = -\sum_j e_j\gamma^j_\mu A^\mu(\mathbf{k},\mathbf{r}). \quad (5)$$

The first term in Eq. (4) is a seagull term. The second and third terms correspond to the s- and u-channels, respectively. The last term is the t-channel contribution and is excluded here due to the duality hypothesis[17].

The contributions from the s-channel resonances to the transition matrix elements can be written as

$$\mathcal{M}_{N^\star} = \frac{2M_{N^\star}}{s-M_{N^\star}(M_{N^\star}-i\Gamma(q))} e^{-\frac{k^2+q^2}{6\alpha^2_{ho}}} \mathcal{A}_{N^\star}, \quad (6)$$

with $k = |\boldsymbol{k}|$ and $q = |\boldsymbol{q}|$ the momenta of the incoming photon and the outgoing meson respectively, $\sqrt{s} \equiv W$ the total energy of the system, $e^{-(k^2+q^2)/6\alpha^2_{ho}}$ a form factor in the harmonic oscillator basis with the parameter α^2_{ho} related to the harmonic oscillator strength in the wave-function, and $M_{N^\star}$ and $\Gamma(q)$ the mass and the total width of the resonance, respectively. The amplitudes $\mathcal{A}_{N^\star}$ are divided into two parts[18]: the contribution from each resonance below 2 GeV, the transition amplitudes of which have been translated into the standard CGLN amplitudes in the harmonic oscillator basis, and the contributions from the resonances above 2 GeV treated as degenerate.

The contributions from each resonance is determined by introducing[19] a new set of parameters $C_{N^\star}$, and the substitution rule $\mathcal{A}_{N^\star} \to C_{N^\star}\mathcal{A}_{N^\star}$, so that $\mathcal{M}^{exp}_{N^\star} = C^2_{N^\star}\mathcal{M}^{qm}_{N^\star}$; with $\mathcal{M}^{exp}_{N^\star}$ the experimental value of the observable, and $\mathcal{M}^{qm}_{N^\star}$ calculated in the quark model[18]. The $SU(6)\otimes O(3)$ symmetry predicts $C_{N^\star} = 0.0$ for $S_{11}(1650)$, $D_{13}(1700)$, and $D_{15}(1675)$ resonances, and $C_{N^\star} = 1.0$ for other resonances in Table 2. Thus, the coefficients $C_{N^\star}$ measure the discrepancies between the theoretical results and the experimental data and show the extent to which the $SU(6)\otimes O(3)$

Table 2. Nucleon resonances with $M \leq 2$ GeV and their assignments in $SU(6) \otimes O(3)$ configurations, masses, and widths.

States	$SU(6) \otimes O(3)$	Mass (GeV)	Width (GeV)
$S_{11}(1535)$	$N(^2P_M)_{\frac{1}{2}-}$		
$S_{11}(1650)$	$N(^4P_M)_{\frac{1}{2}-}$	1.650	0.150
$D_{13}(1520)$	$N(^2P_M)_{\frac{3}{2}-}$	1.520	0.130
$D_{13}(1700)$	$N(^4P_M)_{\frac{3}{2}-}$	1.700	0.150
$D_{15}(1675)$	$N(^4P_M)_{\frac{5}{2}-}$	1.675	0.150
$P_{13}(1720)$	$N(^2D_S)_{\frac{3}{2}+}$	1.720	0.150
$F_{15}(1680)$	$N(^2D_S)_{\frac{5}{2}+}$	1.680	0.130
$P_{11}(1440)$	$N(^2S'_S)_{\frac{1}{2}+}$	1.440	0.150
$P_{11}(1710)$	$N(^2S_M)_{\frac{1}{2}+}$	1.710	0.100
$P_{13}(1900)$	$N(^2D_M)_{\frac{3}{2}+}$	1.900	0.500
$F_{15}(2000)$	$N(^2D_M)_{\frac{5}{2}+}$	2.000	0.490

symmetry is broken in the process investigated here. One of the main reasons that the $SU(6) \otimes O(3)$ symmetry is broken is due to the configuration mixings caused by the one-gluon exchange[20]. Here, the most relevant configuration mixings are those of the two S_{11} and the two D_{13} states around 1.5 to 1.7 GeV. The configuration mixings can be expressed in terms of the mixing angle between the two $SU(6) \otimes O(3)$ states $|N(^2P_M) >$ and $|N(^4P_M) >$, with the total quark spin 1/2 and 3/2. To show how the coefficients C_{N^*} are related to the mixing angles, we express the amplitudes $\mathcal{A}_{N^*}$ in terms of the product of the photo and meson transition amplitudes

$$\mathcal{A}_{N^*} \propto < N|H_m|N^* >< N^*|H_e|N >, \tag{7}$$

where H_m and H_e are the meson and photon transition operators, respectively. For example, for the resonance $S_{11}(1535)$ Eq. (7) leads to

$$\begin{aligned} \mathcal{A}_{S_{11}} \propto < N|H_m(\cos\theta_S|N(^2P_M)_{\frac{1}{2}-} > - \sin\theta_S|N(^4P_M)_{\frac{1}{2}-} >) \\ (\cos\theta_S < N(^2P_M)_{\frac{1}{2}-}| - \sin\theta_S < N(^4P_M)_{\frac{1}{2}-})|H_e|N > . \end{aligned} \tag{8}$$

Then, the configuration mixing coefficients can be related to the configuration mixing angles

$$C_{S_{11}(1535)} = \cos\theta_S(\cos\theta_S - \sin\theta_S), \tag{9}$$

$$C_{S_{11}(1650)} = -\sin\theta_S(\cos\theta_S + \sin\theta_S), \tag{10}$$

$$C_{D_{13}(1520)} = \cos\theta_D(\cos\theta_D - \sqrt{1/10}\sin\theta_D), \tag{11}$$

$$C_{D_{13}(1700)} = \sin\theta_D(\sqrt{1/10}\cos\theta_D + \sin\theta_D). \tag{12}$$

3. Results and Discussion

3.1. *η-photoproduction channel*

we have fitted all $\approx$ 650 data points from recent measurements for both differential cross-sections[21,22,23] and single polarization asymmetries[24]. The adjustable parameters of our models are the ηNN coupling constants and one $SU(6) \otimes O(3)$ symmetry breaking strength coefficient (C_{N^*}) per resonance, except for the resonances $S_{11}(1535)$ and $S_{11}(1650)$ on the one hand, and $D_{13}(1520)$ $D_{13}(1700)$ on the other hand, for which we introduce the configuration mixing angles θ_S and θ_D. The first model includes explicitly

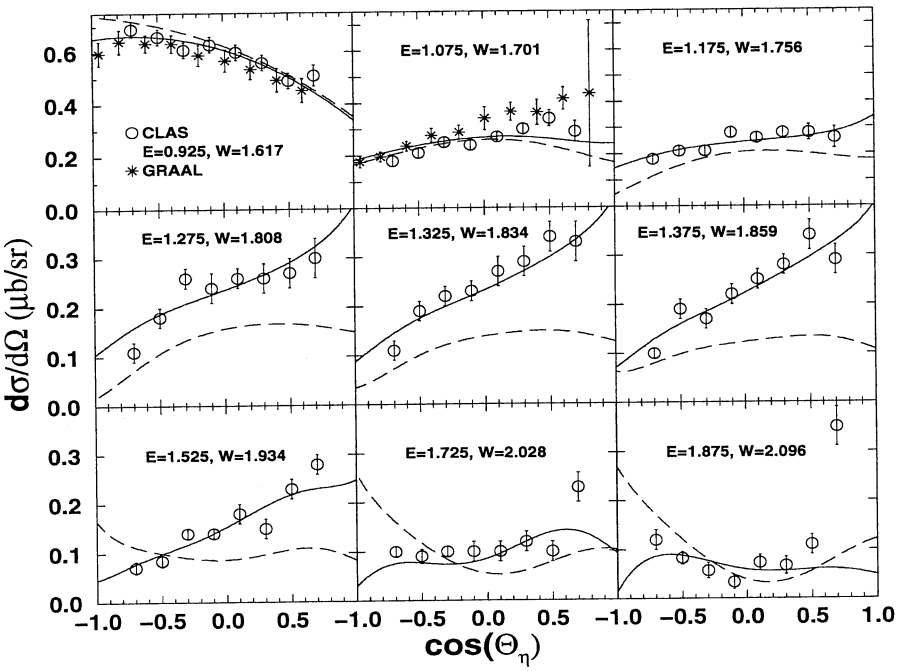

Figure 1. Differential cross section for the process $\gamma p \rightarrow \eta p$: angular distribution at nine incident photon energies (E_γ^{lab}), with the corresponding total center-of-mass energy (W) also given; units are in GeV. The dashed curves are from the model embodying all known three and four star resonances. The full curves show the model including, in addition, a new S_{11} resonance, with M=1.780 GeV and Γ=280 MeV. CLAS (circles) and GRAAL (stars) data are from Refs. [23] and [22], respectively.

all eleven known relevant resonances, mentioned above, with mass below 2 GeV, and the contributions from the known excited resonances above 2

GeV for a given parity. assumed to be degenerate and hence written in a compact form[18]. In Fig. 1, we compare this model (dashed curves) to the data at nine incident photon energies. As shown in our earlier works[17,19], such a model reproduces correctly the data at low energies ($E_\gamma^{lab} \leq 1$ GeV). Above, the model misses the data. A possible reason for these theory/data discrepancies could be that some yet unknown resonances contribute to the reaction mechanism. We have investigated possible rôle played by extra S_{11}, P_{11}, and P_{13} resonances, with three free parameters (namely the resonance mass, width, and strength) in each case.

By far, the most significant improvement was obtained by a third S_{11} resonance, with the extracted values M=1.780 GeV and Γ=280 MeV. The configuration mixing angles came out to be θ_S=12° and θ_D=-35°, in agreement with the Isgur-Karl model[20] and more recent predictions[25].

The outcome of this latter model is depicted in Fig. 1 (full curve) and shows very reasonable agreement with the data, improving the reduced χ^2, on the complete data-base, by more than a factor of 2.

3.2. *Associated strangeness photoproduction channel*

The above formalism has also been used to investigate *all* 1640 recent data points on the differential cross sections[26,27] for the $\gamma p \rightarrow K^+\Lambda$ reaction. The adjustable parameters here are the KYN coupling constant and one $SU(6) \otimes O(3)$ symmetry breaking strength coefficient ($C_{N^\star}$) per nucleon resonance, as in the case of the η-channel (Table 2). Other nucleon resonances and all hyperon resonances in Table 1 are included in a compact form[18] and bear no free parameters.

Figures 2 and 3 show our preliminary results for three excitation functions at $\theta_K^{CM} = 31.79°$, 56.63°, and 123.37° as a function of total center-of-mass energy (W). The choice of the angles is due to the published data by the JLab group[26].

Given the significant discrepencies between the two data sets, the minimization procedure was performed as follows:

(i) Both data sets were fitted *simultaneously*, leading to curve (a) in figures 2 and 3.
(ii) Data sets from JLab[26] and SAPHIR[27] were fitted *separately*. The curve (b) in Fig. 2 is obtained by fitting *only* the JLab data, while the curve (d), Fig. 3, comes out from a fit *only* on the SAPHIR data.
(iii) The curves (a), (b), and (d) correspond to models embodying all known resonances. At this stage, a third S_{11} resonance was intro-

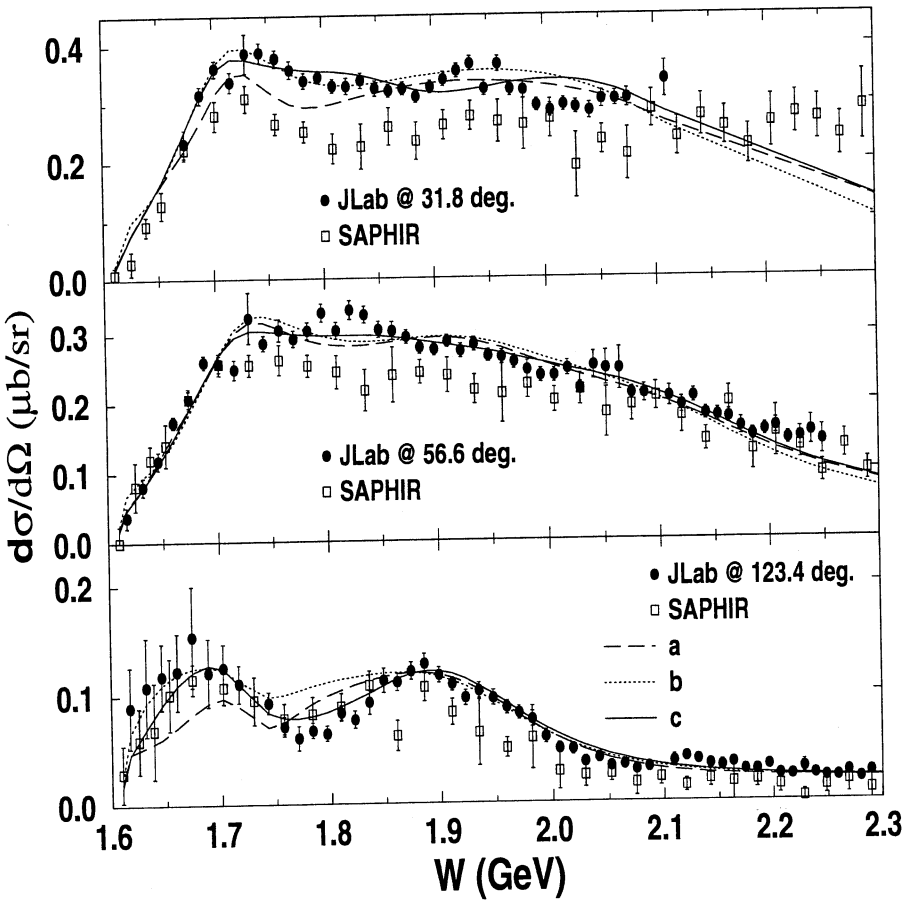

Figure 2. Differential cross section for the process $\gamma p \to K^+\Lambda$ as a function of total center-of-mass energy (W) in GeV. All the curves embody all known resonances. The dashed curve (a) is from a fit to data from both JLab [25] and SAPHIR [26]. The dotted curve (b) is obtained by fitting only JLab data. The full curve (c) corresponds to this latter data set with an additional S_{11} resonance.

duced, in line with the η case. With this additional resonance, the data from JLab and SAPHIR were fitted seperately and the outcomes are the curves (c) and (e) in Figs. 2 and 3, respectively.

The model (a) gives a reduced χ^2 of 3.7 (Table 3). Adding a third S_{11}

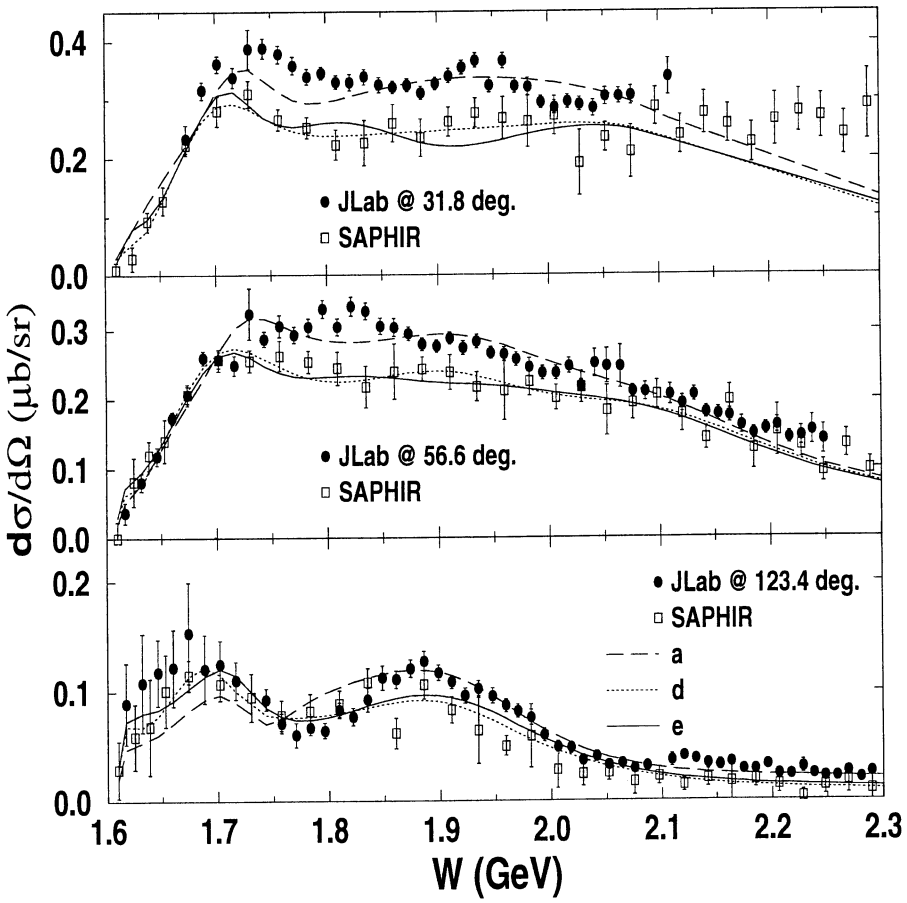

Figure 3. Same as Fig. 2, except for curves (d) and (e). The dotted curve (d) is obtained by fitting only SAPHIR data. The full curve (e) corresponds to this latter data set with an additional S_{11} resonance.

resonance, improves it slightly (χ^2=3.5). However, fitting separately each set of data, shows a significant sensitivity to the introduction of a third S_{11} resonance. Due to this latter new resonance, for the JLab data the χ^2 goes from 3.0 to 1.6, and for the SAPHIR data it gets reduced from 2.1 to 1.4. We notice that in both cases, the SAPHIR data are better reproduced within our approach.

Table 3. Summary of models (a) to (e).

Model	Data	# of data points	Reduced χ^2	3^{rd} S_{11}
a	JLab & SAPHIR	1640	3.7	
b	JLab	920	3.0	
c	JLab	920	1.6	M=1.852 GeV ; Γ=187 MeV
d	SAPHIR	720	2.1	
e	SAPHIR	720	1.4	M=1.835 GeV ; Γ=246 MeV

3.3. *New S_{11} resonance*

Several authors[17,28,29,30,31,32,33,34] have reported on a third S_{11} resonance with a mass around 1.8 GeV (see Table 4). Our chiral constituent quark approach applied to the $\gamma p \to \eta p, K^+\Lambda$ reactions puts the mass in the range of 1.780 to 1.852 GeV and the width between 187 and 280 MeV. This dispersion is, at least partly, due to the discrepancies among data reported by different collaborations. The extracted values for the mass and width from the $\gamma p \to \eta p$ process are consistent with those predicted by the authors of Ref.[29] (M=1.712 GeV and Γ=184 MeV), and our previous findings[17]. Moreover, for the one star $S_{11}(2090)$ resonance[13], the Zagreb group πN and ηN coupled channel analysis[30] produces the following values M = 1.792 $\pm$ 0.023 GeV and Γ = 360 $\pm$ 49 MeV. The BES Collaboration reported[31] on the measurements of the $J/\psi \to p\bar{p}\eta$ decay channel. In the latter work, a partial wave analysis leads to the extraction of the mass and width of the $S_{11}(1535)$ and $S_{11}(1650)$ resonances, and the authors find indications for an extra resonance with M = 1.800 $\pm$ 0.040 GeV, and $\Gamma = 165^{+165}_{-85}$ MeV. A more recent work[32] based on the hypercentral constituent quark model, predicts a missing S_{11} resonance with M=1.861 GeV. Finally, a self-consistent analysis of pion scattering and photoproduction within a coupled channel formalism, iconcludes[33] on the existence of a third S_{11} resonance with M =1.803 $\pm$ 0.007 GeV.

Table 4. Summary of studies on a 3^{rd} S_{11} resonance.

Mass (GeV)	Width (MeV)	Comment	Ref.
1.780	280	CQM applied to $\gamma p \to \eta p$	28; Sec. 3.1
1.835	246	CQM, applied to $\gamma p \to K^+\Lambda$ data from SAPHIR	Sec. 3.2
1.852	187	CQM, applied to $\gamma p \to K^+\Lambda$ data from JLab	Sec. 3.2
1.730	180	KY molecule	29
1.792	360	πN and ηN coupled-channel analysis	30
1.800	165	J/Ψ decay	31
1.861		Hypercentral CQM	32
1.846		Pion photoproduction coupled-channel analysis	33

4. Summary and Concluding remarks

In this contribution, the results of a chiral constituent quark model have been compared with the most recent published data on the $\gamma p \to \eta p, K^+\Lambda$ processes, with emphasize on a third S_{11} resonance. Our results are consistent with findings by other authors[29,30,31,32,33], showing evidence for such a new resonance, with $M \approx 1.8$ GeV and $\Gamma \approx 250$ MeV.

In the case of the η photoproduction channel, we need to extend our analysis to the very recent data from ELSA[35].

The associated strangeness production channel suffers at the present time from discrepancies between the two copious data set from JLab and SAPHIR. New data from GRAAL will hopefully provide us with a better vision of the experimental situation. Within our approach, a more comprehensive interpretation of the $K^+\Lambda$ channel is underway with respect to the polarization observables[36], as well as to the observables[26,27] of the $\gamma p \to K^+\Sigma^\circ$.

To go further, the coupled channel effects[37,38,39,40,41,42] have to be considered. The effect of the multi-step process $\gamma p \to \pi N \to K^+\Lambda$ has been reported[40] to be significant at the level of inducing 20% changes on the total cross section of the direct channel ($\gamma p \to K^+\Lambda$). The dynamics of the intermediate states $\pi N \to KY$, as well as final states interactions $KY \to KY$, with $Y \equiv \Lambda, \Sigma$ have been recently studied[41] within a dynamical coupled-channel model of meson-baryon interactions. Those efforts deserve to be extended to the multi-step processes

$$\gamma p \to \pi N \to \eta p \ , \ K^+\Lambda \ , \ K^+\Sigma^\circ \ , \ K^\circ\Sigma^+,$$

and also embody the final state interactions.

It is a pleasure for me to thank K.H. Glander and R. Schumacher for having provided me with the complete set of SAPHIR and JLab data, respectively, prior to publication. I am indebted to my collaborators W.T. Chiang, C. Fayard, T.-S. H. Lee, Z. Li, T. Mizutani, and F. Tabakin.

References

1. See e.g. W.J. Briscoe, R.A. Arndt, I.I. Strakovski, R.L. Workman, *nucl-ex/0310003*.
2. N.C. Mukhopadhyay, J. F. Zhang, and M. Benmerrouche, *Phys. Lett.* **B3**, 1 (1995); M. Benmerrouche, N.C. Mukhopadhyay, J. F. Zhang, *Phys. Rev.* **D51**, 3237 (1995); N.C. Mukhopadhyay, N. Mathur, *Phys. Lett.* **B444**, 7 (1998); R.M. Davidson, N. Mathur, N.C. Mukhopadhyay, *Phys. Rev.* **C62**, 058201 (2000).
3. W.-T. Chiang, S.N. Yang, L. Tiator, D. Drechsel, *Nucl. Phys.* **A700**, 429 (2002); W.-T. Chiang *et al.*, *Phys. Rev.* **C68**, 045202 (2003).
4. V.A. Tryasuchev, *Phys. Atom. Nucl.* **65**, 1673 (2002).
5. I.G. Aznauryan, *Phys. Rev.* **C68**, 065204 (2003).
6. S.S. Hsiao, S.R. Cotanch, *Phys. Rev.* **C28**, 1668 (1983); R.A. Williams, C.R. Ji, S.R. Cotanch, *Phys. Rev.* **C46**, 1617 (1992).
7. R.A. Adelseck, C. Bennhold, L.E. Wright, *Phys. Rev.* **C32**, 1681 (1985); T. Mart, C. Bennhold, *Phys. Rev.* **C61**, 012201 (2000).
8. R.A. Adelseck, B. Saghai, *Phys. Rev.* **C42**, 108 (1990); J.C. David, C. Fayard, G.H. Lamot, B. Saghai, *Phys. Rev.* **C53**, 2613 (1996).
9. B.S. Han, M.K. Cheoun, K.S. Kim, I-T. Cheon, *Nucl. Phys.* **A691**, 713 (2001).
10. S. Janssen, D.G. Ireland, J. Ryckebusch, *Phys. Lett.* **B562**, 51 (2003); S. Janssen, J. Ryckebusch, T. Van Cauteren, *Phys. Rev.* **C67**, 052201 (2003); D.G. Ireland, S. Janssen, J. Ryckebusch, *nucl-th/0312103*.
11. B. Saghai, *nucl-th/0310025*.
12. M. Benmerrouche, R.M. Davidson, N.C. Mukhopadhyay, *Phys. Rev.* **C39**, 2339 (1989); T. Mizutani, C. Fayard, G.H. Lamot, B. Saghai, *Phys. Rev.* **C58**, 75 (1998).
13. K. Hagiwara *et al.*, Particle Data Group, *Phys. Rev.* **D66**, 010001 (2002).
14. B. Saghai, *nucl-th/0105001*.
15. See e.g. S. Capstick, W. Roberts, *Prog. Part. Nucl. Phys.* **45**, 5241 (2000); and references therein; S. Capstick, these proceedings.
16. A. Manohar, H. Georgi, *Nucl. Phys.* **B234**, 189 (1984).
17. B. Saghai, Z. Li, *Eur. Phys. J.* **A11**, 217 (2001).
18. Z. Li, H. Ye, M. Lu, *Phys. Rev.* **C56**, 1099 (1997).
19. Z. Li, B. Saghai, *Nucl. Phys.* **A644**, 345 (1998).
20. N. Isgur, G. Karl, *Phys. Lett.* **B72**, 109 (1977); N. Isgur, G. Karl, R. Koniuk, *Phys. Rev. Lett.* **41**, 1269 (1978).
21. B. Krusche *et al.*, *Phys. Rev. Lett.* **74**, 3736 (1995).
22. F. Renard *et al.* (The GRAAL Collaboration), *Phys. Lett.* **B528**, 215 (2002).
23. M. Dugger *et al.* (The CLAS Collaboration), *Phys. Rev. Lett.* **89**, 222002 (2002).
24. A. Bock *et al.*, *Phys. Rev. Lett.* **81**, 534 (1998); J. Ajaka *et al.*, *ibid* **81**, 1797 (1998).
25. He Jun, Dong Yu-bing, *Phys. Rev.* **D68** 017502 (2003); J. Chizma, G. Karl, *ibid* **D68** 054007 (2003).
26. J.W.C. McNabb *et al.* (The CLAS Collaboration), *Phys. Rev.* **C69**, 042201

(2004).
27. K.H. Glander *et al.* (The SAPHIR Collaboration), *Eur. Phys. J.* **A19**, 251 (2004); K.H. Glander, these proceedings.
28. B. Saghai, Z. Li, *nucl-th/0305004*.
29. Z. Li, R. Workman, *Phys. Rev.* **C53**, R549 (1996).
30. A. Švarc, S. Ceci, *nucl-th/0009024*; A. Švarc, these proceedings.
31. J.-Z. Bai *et al.*, *Phys. Lett.* **B510**, 75 (2001).
32. M.M. Giannini, E. Santopinto, A. Vassallo, *nucl-th/0302019*.
33. G.-Y Chen, S. Kamalov, S.N. Yang, D. Drechsel, L. Tiator *Nucl. Phys.* **A723**, **447** (2003); S. Kamalov, these proceedings.
34. V.A. Tryasuchev, *Phys. Atom. Nucl.* **67**, 427 (2004).
35. V. Credé *et al.*, (CB-ELSA Collaboration), *hep-ex/0311045*.
36. R.T.G. Zegers *et al.* (The LEPS Collaboration), *Phys. Rev. Lett.* **91**, 092001 (2003).
37. J. Caro Ramon, N. Kaiser, S. Wetzel, W. Weise, *Nucl. Phys.* **A672**, 249 (2000).
38. J.A. Oller, E. Oset, A. Ramos, *Prog. Part. Nucl. Phys.* **45**, 157 (2000).
39. G. Penner, U. Mosel, *Phys. Rev.* **C66**, 055212 (2002).
40. W.-T Chiang, F. Tabakin, T.-S. H. Lee, B. Saghai, *Phys. Lett.* **B517**, 101 (2001).
41. W.-T Chiang, B. Saghai, F. Tabakin, T.-S. H. Lee, *nucl-th/0404062*, to appear in *Phys. Rev.* **C**.
42. T.-S. H. Lee, these proceedings.